ELSEVIER

Catalysis Today 36 (1997) 71–79

CATALYSIS TODAY

Copper–zirconia catalysts for NO–CO reactions

Yasuaki Okamoto *, Hideki Gotoh

Department of Chemical Engineering, Faculty of Engineering Science, Osaka University, Toyonaka, Osaka 560, Japan

Abstract

Copper–zirconia catalysts have shown high activities and selectivities for a NO–CO reaction at low temperature. Highly active Cu(L) species are produced by replacing the terminal OH groups of the ZrO_2 surface and assigned to atomically dispersed Cu species. The deactivation of Cu(L) species took place in two steps; relatively rapid activity loss and subsequent slow deterioration. Treatments with 1% NO regenerated the deactivated Cu/ZrO_2 at a much lower temperature than treatments with 5% O_2. The addition of Fe to Cu/ZrO_2 was found to dramatically improve the catalytic performances; the activity and selectivity to N_2 at low temperature and catalytic stability. The mechanisms of reaction, deactivation, and regeneration are proposed.

Keywords: Cu/ZrO_2 catalyst; NO–CO reaction; Deactivation; Regeneration; Catalytic synergy

1. Introduction

The abatement of NO_x from effluent gases is one of the most important subjects to be solved for the protection of the environments [1]. Catalytic reduction of NO_x by CO is considered to be the most fundamental reaction in the conversion of automobile exhaust gases, i.e., CO, NO_x, hydrocarbons, and oxidants [2]. The reduction of NO by CO is catalyzed by precious metals, in particular Rh as used in three way conversion catalysts [3]. The scarcity and high price of Rh, however, promoted the investigations to develop novel catalyst systems; low-Rh content or non-Rh catalysts such as ZnO-supported Pt catalysts [4,5] and the catalysts using the first transition metals as main catalytic components.

Supported Cu catalysts have recently received much attention as NO conversion catalysts; Cu-exchanged zeolites [6], in particular Cu-ZSM-5, for selective catalytic reduction of NO with hydrocarbons in the presence of O_2 and for direct decomposition of NO into N_2 and O_2. Perovskite catalysts [7–10] containing Cu show catalytic activities for the direct decomposition of NO and for a NO reduction by CO. Copper oxides supported on metal oxides also exhibit activities for NO–CO reactions. Bauerle et al. [11] showed that Al_2O_3-supported CuO and $CuCr_2O_4$ exhibited catalytic activities for a NO–CO reaction at $< 320°C$ in an excess of CO. Okamoto et al. [12] have recently reported in a preliminary paper that ZrO_2-supported Cu and Cu–Fe catalysts show high activities and selectivities for a NO–CO reaction to N_2 at $> 170°C$. Boccuzzi et al. [13] suggested a low temperature activity of Cu/TiO_2 for the NO

---

* Corresponding author. Present address: Department of Materials Science, Shimane University, Matsue 960, Japan.

PII S0920-5861(96)00198-8

reduction by CO. Despite being one of the most fundamental NO removal reactions, NO–CO reactions over supported Cu catalysts have never been fully investigated up to now. In the present study, the catalytic properties and stability of ZrO_2-supported Cu catalysts were studied in detail for NO–CO reactions. The addition of Fe oxide was found to dramatically improve the catalytic performances of the Cu/ZrO_2 catalysts.

2. Experimental

2.1. Catalyst Preparation

Cu/ZrO_2 catalysts were prepared by impregnating ZrO_2 with aqueous solutions of $Cu(CH_3COO)_2$. After drying at 110°C for 20h, the catalysts were calcined in air at 700°C for 1h using an electric furnace. Zirconia was provided by Daiichi Kigenso Co. Ltd. (EP, 1.38 wt% Hf, 25 m^2/g). Other kinds of ZrO_2 were also examined for comparison. Copper catalysts supported on TiO_2, SiO_2, and Al_2O_3 were also prepared by an impregnation method using $Cu(CH_3COO)_2$, followed by drying at 110°C for 20h and a subsequent calcination at 700°C for 1h. TiO_2 (JRC-TIO-4, 50 m^2/g), SiO_2 (JRC-SIO-4, 347 m^2/g), and Al_2O_3 (JRC-ALO-4, 177 m^2/g) were supplied by the Catalysis Society of Japan as reference catalysts.

$Cu–Fe/ZrO_2$ catalysts were prepared by co-impregnating ZrO_2 (EP) with $Cu(CH_3COO)_2$ and $Fe(NO_3)_3$ aqueous solutions, followed by drying at 110°C for 20h. Fe/ZrO_2 catalysts were prepared using $Fe(NO_3)_3$. The catalysts were calcined at 700°C for 1h.

2.2. Reaction procedures

A NO–CO reaction was carried out using a fixed bed flow reactor (0.1 g cat.). The flow rates of the reaction gases were controlled using mass flow meters (Ueshima-Brooks 5850E). The concentrations of CO and NO in a He stream (20 cm^3/min) were identical and 2500 ppm (GHSV; 12,000 h^{-1}) otherwise noted. The catalyst was treated at 400°C for 1h in a stream of 5% O_2 prior to the reaction. After the temperature was decreased to room temperature, the O_2-stream was completely replaced by the reaction gas. The reaction temperature was increased at a rate of 3°C/min from room temperature to 500°C. The reaction gas was analyzed by an on-line gas chromatography. A catalyst activity was also measured at a fixed reaction temperature.

2.3. IR Study

FTIR spectra of Cu/ZrO_2 were measured using an in situ cell at room temperature on a Shimazu FTIR 8200PC. The catalyst was pressed into a self-supporting disc. The catalyst sample was evacuated ($< 10^{-5}$ Torr) at 300°C for 1h and subsequently treated with 20 Torr of O_2 for 20 min at the same temperature, followed by degassing for 1 min.

3. Results and discussion

3.1. Support effect

The support effects on the performances of Cu catalysts were examined for the NO–CO reaction to find the most efficient catalyst system, in particular at low temperature. Fig. 1 shows the NO conversions over the supported Cu catalysts containing 1 wt% Cu as a function of the reaction temperature. ZrO_2 – and TiO_2-supported Cu catalysts were found to exhibit considerable activities at 150–200°C and the activity minima, especially with Cu/TiO_2 were observed as shown in Fig. 1. The catalytic activities of Cu/SiO_2 and Cu/Al_2O_3 were very low under the present preparation conditions. At 5 wt% Cu, the activity sequence as defined by the 50% conversion of NO was as follows; $Al_2O_3 \sim ZrO_2 > SiO_2 > SiO_2–MgO > TiO_2 \gg SiO_2–Al_2O_3$ [12]. ZrO_2- and TiO_2-supported

Cu catalysts showed low temperature activities at < 200°C as observed in Fig. 1. Of the supports examined in the present and previous studies [12], ZrO_2 was found to provide the most active Cu catalysts for the NO–CO reaction, in particular, at low temperature. Accordingly, in the present study the properties of Cu/ZrO_2 catalysts were studied in detail. Cu/ZrO_2 catalysts also showed high activities for the oxidation of CO [12,14]. Recently, Cu/ZrO_2 was reported to be effective for the NO reduction by hydrocarbons in the presence of O_2 [15]. The combinations of Cu and ZrO_2 have been reported to exhibit high activity and selectivity for the methyl alcohol formation from CO_2 and H_2 [16–20].

The conversion of CO and the conversion of NO to N_2O over the 1wt% Cu/ZrO_2 catalyst are compared in Fig. 2 with the NO conversion. Nitric oxide is converted predominantly to N_2O at < 150°C and selectively to N_2 at > 250°C. On the basis of the N_2O concentration versus W/F and the results in Fig. 2, it is concluded that the reduction of NO to N_2 proceeds through N_2O as an intermediate. It is worthy to note that the conversion of CO prevailed that of NO at < 150°C and at > 200°C, indicating that the reactions of NO take place on reduced Cu sites. It is obvious from Fig. 1 and Fig. 2 that there are two kinds of Cu species with different activities for the NO–CO reaction; Cu species active at a low temperature (< 200°C) and at a high temperature (> 250°C). These Cu species are denoted Cu(L) and Cu(H), respectively.

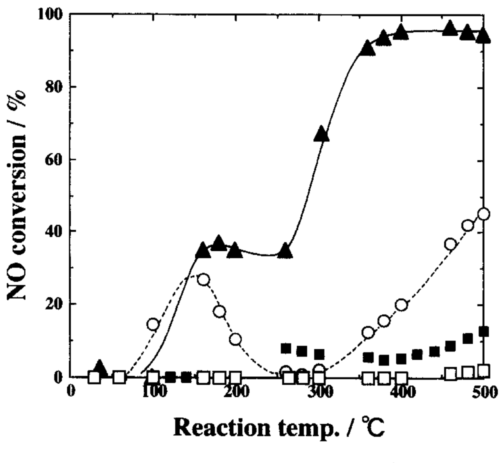

Fig. 1. Activity of a supported Cu catalyst (1 wt% Cu) for NO–CO reaction as a function of reaction temperature. ▲: Cu/ZrO_2, ○: Cu/TiO_2, ■: Cu/Al_2O_3, and □: Cu/SiO_2.

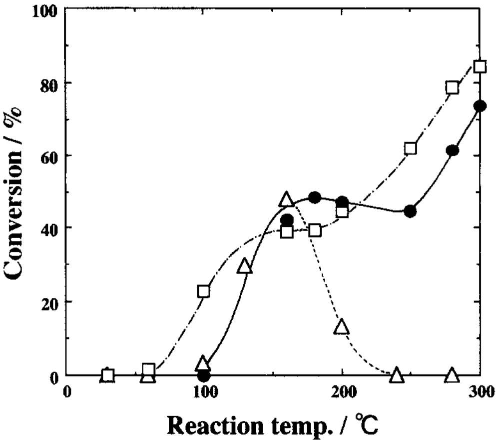

Fig. 2. Catalytic behavior of Cu/ZrO_2 (1 wt% Cu) for NO–CO reaction. ●: NO conversion, □: CO conversion, and △: NO conversion to N_2O.

Fig. 3 shows the dependence of the activity of Cu/ZrO_2 for a NO–CO reaction (NO; 2500 ppm and CO; 2000 ppm) upon the Cu loading. The NO conversion of the low temperature peak linearly increased up to 1 wt% Cu and almost levelled off at a further addition of Cu, indicating that the amount of Cu(L) species is limited. At a high temperature, 400–500°C, the NO conversion increased as the Cu content in-

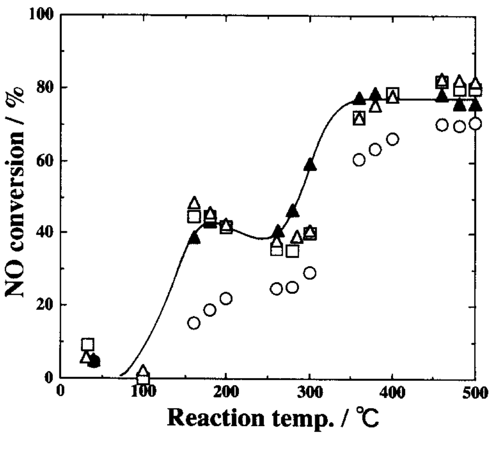

Fig. 3. Activity of Cu/ZrO_2 for NO–CO reaction as a function of Cu content. ○: 0.5 wt%, ▲: 1.0 wt%, □: 3 wt%, and △: 5 wt%.

creased (note that the maximum NO conversion is 80% because of the gas composition so long as the decomposition of NO does not occur). The maximum activity was reached at 1 wt% Cu at the medium temperature region, 250–350°C (vide infra). The low temperature activity of Cu/ZrO_2 (1 wt% Cu) was found to increase in proportion to the surface area of the ZrO_2 support (15–25 m^2/g) and to be independent of Hf content (1.38–1.78 wt%). Cu/ZrO_2 catalysts prepared using $Cu(NO_3)_3$ as a starting material and calcined at 700°C showed the same activities as those of the catalysts from $Cu(CH_3COO)_2$. The calcination temperature (300–700°C) did not affect the surface area and the activity of 1 wt% Cu/ZrO_2 prepared using $Cu(CH_3COO)_2$. The findings that the amount of Cu(L) is limited ($3–4 \times 10^{14}$ Cu cm^{-2} at most), which is lower than a half of the surface O^{2-} anions, suggest that Cu(L) species is atomically dispersed Cu^{2+} species. It is inferred that the Cu species exceeding a certain coverage of the support surface form a highly dispersed CuO attributable to Cu(H) species.

Two kinds of Cu species were also observed for Cu/TiO_2 as illustrated in Fig. 1. The activity around 150°C was significantly lower when 1 wt% Cu/TiO_2 was calcined at 300–500°C, suggesting that the Cu(L) species are formed by specific interactions with the TiO_2 surface. The low activities at 200–300°C of Cu/ZrO_2 and Cu/TiO_2 are considered to be ascribed to the deactivation of Cu(L) species as discussed below.

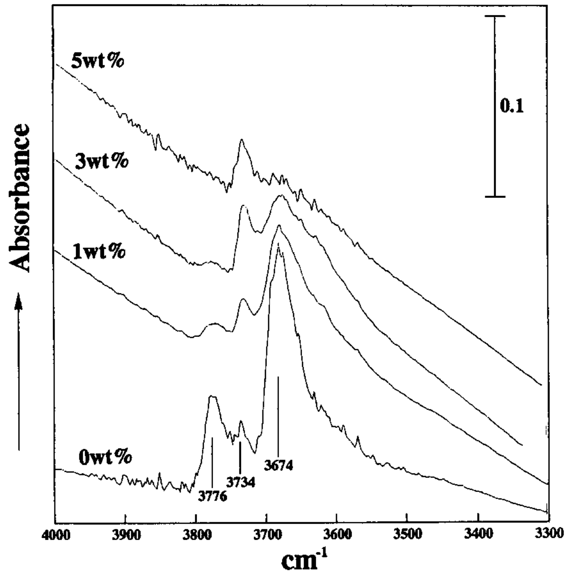

Fig. 4. FTIR spectra of Cu/ZrO_2. Cu content is shown in the figure.

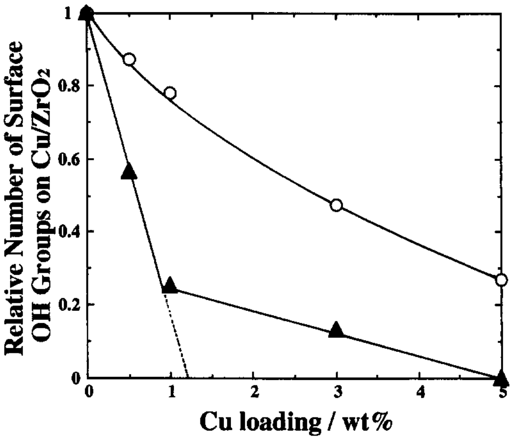

Fig. 5. Dependences of the relative number of surface OH groups of Cu/ZrO_2 on Cu loading. ▲: 3776 cm^{-1} and ○: 3674 cm^{-1}.

The interaction modes of Cu species in the fresh Cu/ZrO_2 catalysts with the ZrO_2 surface were estimated on the basis of the IR study of Cu/ZrO_2. Fig. 4 shows the IR spectra of hydroxyl groups of Cu/ZrO_2 as a function of the Cu content. Three kinds of OH groups were observed on ZrO_2 at 3776 and 3674 cm^{-1}, which are assigned to the terminal and bridging OH groups on the ZrO_2 surface, respectively [21,22], and at 3734 cm^{-1}. The last band has not been reported before. Deuteration of ZrO_2 by use of D_2O confirmed that the band at 3734 cm^{-1} is also due to surface hydroxyl groups. It may be attributed to the OH groups attached to surface HfO_2.

The intensities of the surface OH groups on ZrO_2 decreased as the Cu content increased. This indicates that Cu^{2+} species are accommodated on the ZrO_2 surface by replacing the surface OH groups. The terminal OH groups at 3776 cm^{-1} are apparently consumed more preferentially than the bridging OH groups at 3674

cm^{-1}. The OH groups at 3734 cm^{-1} remained intact, suggesting that they are almost inactive for the interactions with the Cu species. The IR intensities of the surface OH groups of Cu/ZrO_2 relative to those of pure ZrO_2 are plotted in Fig. 5 as a function of the Cu loading. An extrapolation of the consumption curve of the 3776 cm^{-1} band intensity intersects the abscissa around 1 wt% Cu. Therefore, it is concluded that Cu(L) species are formed by the reactions with the terminal OH groups of ZrO_2. The moderate decrease in the IR band intensity of the OH groups at 3674 cm^{-1} over a wide range of Cu loadings suggests that the bridging OH groups are mainly involved in the formation of Cu(H) species.

3.2. Deactivation of Cu/ZrO_2

The catalytic activity of Cu(L) species for the NO–CO reaction was easily destroyed. Fig. 6 illustrates the hysteresis behaviour of Cu(L) species for the NO–CO reaction. The activity was found to be greatly decreased when the activity was measured as the reaction temperature was decreased (3°C/min) after the temperature had been raised up to 300°C in the stream of NO–CO. The activity stayed low and the activity peak around 170°C did not appear even when the reaction temperature was increased again (not shown in Fig. 6 for brevity). The activity was also decreased by treating the fresh Cu/ZrO_2 catalyst at 250°C with 1% CO for 1 h, suggesting that Cu(L) species lose the low temperature activity under the reducing conditions. According to an X-ray absorption fine structure (XAFS) study [23], it is shown that Cu^0 species are formed in both activated and deactivated catalysts and that formation of Cu^+ was detected only at < 100°C.

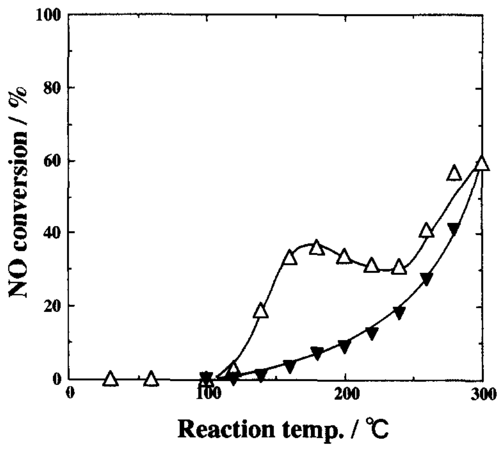

Fig. 6. Hysteresis of 1 wt% Cu/ZrO_2 for NO–CO reaction. Activity was measured with increasing (△) or decreasing (▼) temperature.

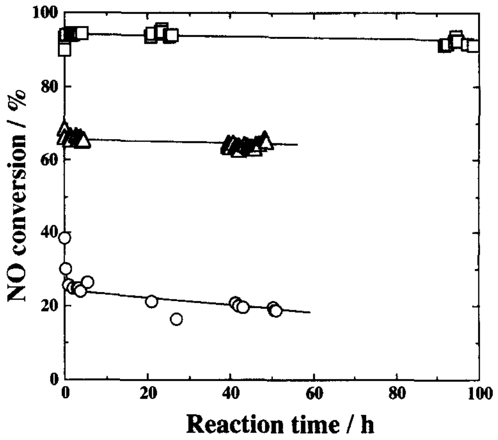

Fig. 7. Catalytic activities of 1 wt% Cu/ZrO_2, 2 wt% Fe/ZrO_2, and 1 wt% Cu-2 wt% Fe/ZrO_2 for the NO–CO reaction at 250°C as a function of reaction time. ○: Cu/ZrO_2, △: Fe/ZrO_2, and □: $Cu–Fe/ZrO_2$.

Fig. 7 presents the activity change of Cu/ZrO_2 (1 wt% Cu) for the NO–CO reaction at 250°C with the reaction time. The activity dropped rapidly in a few hours, accompanied by a gradual activity decay. The rapid deactivation apparently corresponds to the activity hysteresis in Fig. 6.

3.3. Reaction and deactivation mechanisms

The above results are summarized as follows; (1) Cu(L) species are formed by the interactions with the terminal OH groups of the ZrO_2 surface, (2) The catalytic hysteresis is observed for Cu(L) species, (3) The deactivation occurs under the reducing conditions, (4) Cu^0 species was predominant at > 150°C in a 1% CO stream [23], and (5) The activity of the Cu(L) species deteriorates rapidly during the initial stage of the NO–CO reaction and is accompanied by a slow deactivation. The rate equations for the NO conversion over the fresh and deactivated Cu(L) species were found to be presented by equations (1) and (2), respectively.

$$r_F = k_F P_{NO}^{0.85} P_{CO}^{0} \text{ at } 250°\text{C}, \quad (1)$$

$$r_D = k_D P_{NO}^{1.0} P_{CO}^{-0.1} \text{ at } 250°\text{C}. \quad (2)$$

They are essentially identical and the adsorption or decomposition of NO on Cu^0 sites produced by the reduction with CO is considered to be the rate limiting step. The prevailing reduction of Cu species by CO in Fig. 2 are consistent with the rate equations.

The reaction and deactivation mechanisms are proposed in Fig. 8. Oxidic Cu(L) species (**1**) are reduced by CO, forming atomically dispersed Cu^0 species (**2**) and CO_2. A nitric oxide molecule adsorbs on species (**2**) and a mononitrosyl species (**3**) is produced. Another NO molecule attacks species (**3**), producing N_2O through unstable dinitrosyl intermediates. Species (**1**) is formed again, constituting a catalytic cycle. Nitrous oxide is considered to react with species (**2**), forming N_2 and species (**1**). A redox cycle involving Cu^{2+} and Cu^0 is proposed, since the activity generates as Cu is formed [23]. The mechanism in Fig. 8 is compatible with the rate equation (1).

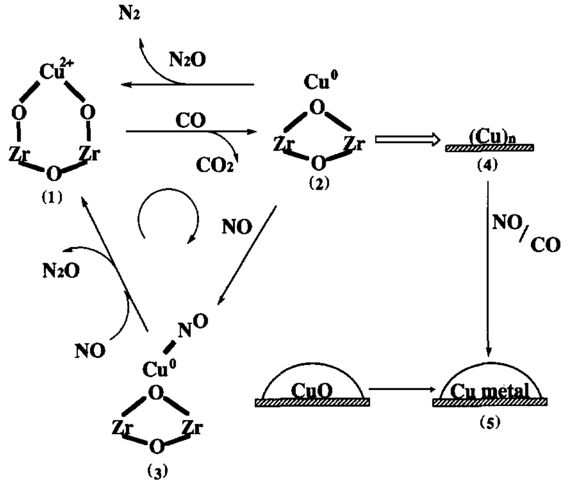

Fig. 8. Proposed reaction and deactivation mechanisms of Cu/ZrO_2 for NO–CO reaction.

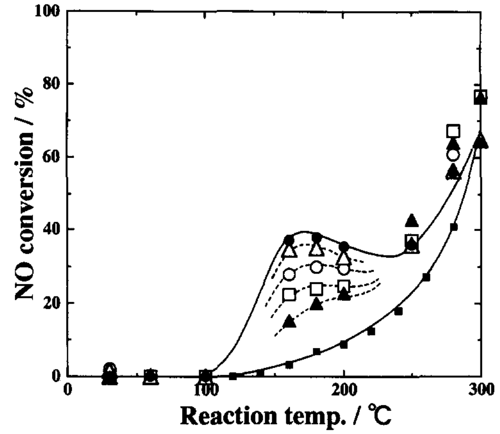

Fig. 9. Regeneration of Cu/ZrO_2 by NO treatment (1% in He). Cu/ZrO_2 had been deactivated by the temperature programmed NO–CO reaction up to 300°C. ●: Fresh and ■: deactivated Cu/ZrO_2. Treatment temperature; ▲: 100, □: 150, ○: 200, and △: 250°C.

The rapid deactivation and catalytic hysteresis are proposed to be the formation of Cu metal clusters (**4**) by agglomerations of atomically dispersed, unstable Cu^0 species (**2**). The subsequent slow deterioration of the activity is caused by the sintering of highly dispersed Cu metal clusters. The resultant Cu metal particles (**5**) show catalytic activities for the NO–CO reaction at > 250°C. Cu(H) species are considered to be dispersed CuO and to form metal particles during the reaction. The fact in Fig. 2 that CO is consumed more than NO at > 250°C may be ascribed to the reductions or activations of Cu(H) species.

As shown in Fig. 3, 1 wt% Cu/ZrO_2 exhibits the highest activity between 250–400°C. This high activity may be ascribed to the relatively high dispersion of Cu metal clusters (**4**) due to the low Cu content.

3.4. Regeneration of deactivated Cu/ZrO_2

It was found that the deactivated Cu/ZrO_2 catalysts were regenerated by treating with O_2 or NO. Fig. 9 shows the effects of the treatment temperature of Cu/ZrO_2, which had been deac-

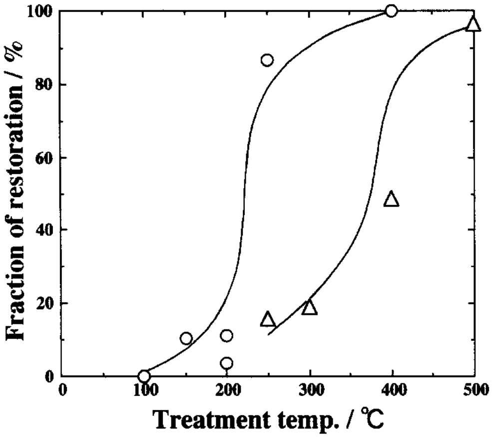

Fig. 10. Fraction of restored activity of Cu/ZrO_2 for NO–CO reaction at 200°C as a function of treatment temperature. △: O_2-treatment and ○: NO-treatment.

tivated by the temperature programmed NO–CO reaction up to 300°C, in a stream of 1% NO upon the catalytic activity at a low temperature. It is conjectured from the colour change of the catalyst with the NO treatment that Cu species are oxidized by the treatment. Obviously, the activity recovered more as the treatment temperature increased. The extent of activity restoration is represented here by the ratio of the activity of recovered Cu(L) to that of the fresh Cu(L), that is, $(k-k_D)/(k_F-k_D)$, where k_F, k_D, and k are the rate constants of the fresh, deactivated, and partially regenerated Cu/ZrO_2. These values were calculated using the rate Eq. (1). Fig. 10 presents the extent of activity restoration by the treatment of 1% NO or 5% O_2 as a function of the treatment temperature. The low temperature activity of Cu/ZrO_2 was significantly recovered at 250°C by the NO treatment, whereas it was restored only at 500°C by the O_2 treatment. It is noteworthy that the deactivated Cu(L) species are much more readily regenerated by the NO treatment than the O_2 treatment. These results indicate that the oxidation mechanism of deactivated Cu species and thereby the structure and dispersion of the oxidized Cu species are different between the NO and O_2 treatments.

The regeneration mechanism is proposed in Fig. 11. In the case of the O_2 treatment at < 400°C, Cu metal clusters or particles are simply oxidized to dispersed CuO, that is, Cu(H) species, which exhibit low catalytic activities for the NO–CO reaction. At > 500°C, the dispersed CuO is considered to react with the ZrO_2 surface, forming species (**1**) again. It is well known that solid–solid reactions at high temperature induce the dispersion of agglomerated species over the support, e.g., MoO_3–Al_2O_3 [24,25].

On the other hand, NO is proposed to disrupt the metal particles, producing isolated Cu^0–NO species, as illustrated in Fig. 11. The Cu^0–NO species, which is identical with species (**3**) in Fig. 8, reacts with another NO molecule and

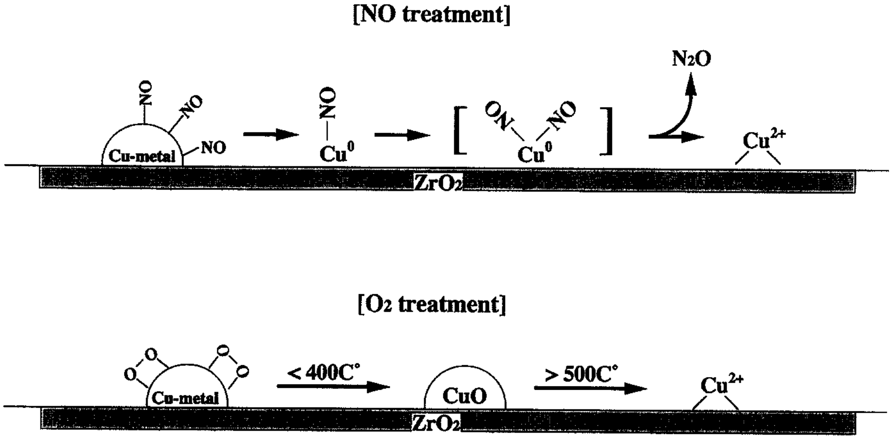

Fig. 11. Proposed regeneration mechanisms of Cu/ZrO_2.

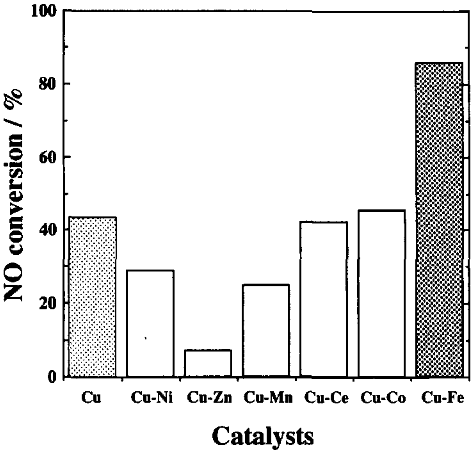

Fig. 12. Catalytic activities of Cu–M/ZrO_2 (1 wt% Cu and 1 wt% M) for NO–CO reaction at 200°C.

subsequently forms N_2O and the original oxidic species (1). Adsorption-induced restructuring of metal particles have been reported for highly dispersed Rh [26] and Ru [27] metal particles supported on Al_2O_3. Carbon monoxide induces the disintegration of Rh and Ru metal particles even at room temperature and the corresponding isolated dicarbonyl, monovalent species are reversibly formed.

3.5. Catalytic Properties of Cu–Fe / ZrO_2

In order to improve the catalytic properties of Cu/ZrO_2 catalysts, the effects of an additive to Cu/ZrO_2 (1 wt% Cu) were examined. The NO conversion at 200°C is summarized in Fig. 12 for Cu–M/ZrO_2 possessing 1 wt% Cu and 1 wt% M. It is evident that the addition of Fe greatly increases the low temperature activity of Cu/ZrO_2, while other metal oxides, in particular ZnO, decrease the activity. Fig. 13 shows the dependencies of the NO conversion and the selectivity to N_2 upon the Fe loading, indicating that the highest performances are attained at 2 wt% Fe for 1 wt% Cu/ZrO_2.

The catalytic activities of 1 wt% Cu/ZrO_2, 2 wt% Fe/ZrO_2, and 1 wt% Cu–2 wt% Fe/ZrO_2 are compared in Fig. 14 for the NO–CO reaction. Cu–Fe/ZrO_2 was found to exhibit much higher activity than the simple sum of the activities of the corresponding Cu/ZrO_2 and Fe/ZrO_2, indicating that catalytic synergies are generated for the NO–CO reaction between Cu and Fe supported on ZrO_2. The rate equations of Fe/ZrO_2 and Cu–Fe/ZrO_2 were found to be presented by equations (3) and (4), respectively.

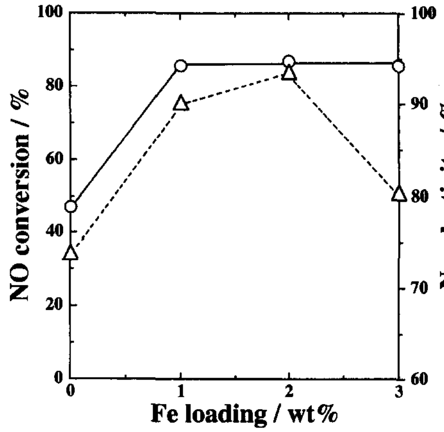

Fig. 13. Effect of Fe content on the activity and selectivity to N_2 of Cu–Fe/ZrO_2 for NO–CO reaction at 250°C. ○: NO conversion and △: selectivity to N_2.

$$\mathrm{Fe/ZrO_2}: r = kP_{\mathrm{CO}}^{0.91}P_{\mathrm{NO}}^{-0.40}\ \text{at}\ 250°\mathrm{C}, \tag{3}$$

$$\mathrm{Cu-Fe/ZrO_2}: r = kP_{\mathrm{CO}}^{0.9}P_{\mathrm{NO}}^{0.8}\ \text{at}\ 250°\mathrm{C}. \tag{4}$$

In the case of Fe/ZrO_2, the rate determining step is suggested to be a partial reduction of highly dispersed Fe_2O_3 species, while in the case of Cu/ZrO_2 the adsorption or decomposition of NO is suggested to be the rate limiting step on the basis of the rate Eqs. (1) and (2). Eq.

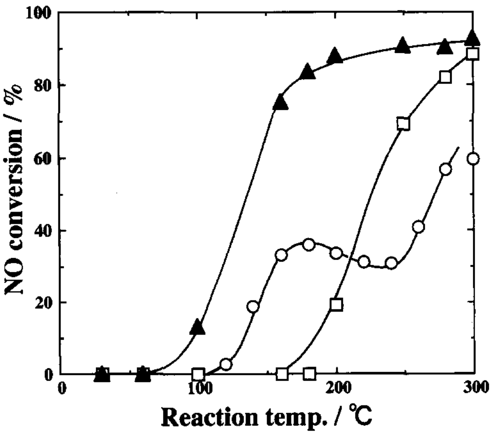

Fig. 14. Activities of Cu/ZrO_2, Fe/ZrO_2, and Cu–Fe/ZrO_2 for NO–CO reaction as a function of reaction temperature. ○: Cu/ZrO_2, □: Fe/ZrO_2, and ▲: Cu–Fe/ZrO_2.

(4) for the ternary system, on the other hand, suggests that both Cu and Fe are involved in the catalytic cycle of the NO reduction by CO. The mechanisms of the NO–CO reaction and of the synergy generation between Cu and Fe are under study now.

Fig. 7 compares the catalytic stability of Cu–Fe/ZrO_2 for the NO–CO reaction at 250°C with those of the component catalysts. Evidently, Cu–Fe/ZrO_2 shows highly stabilized activity as Fe/ZrO_2 does. Thus, Cu–Fe/ZrO_2 possesses both the high activity and selectivity particularly at low temperature of Cu/ZrO_2 and the high stability of Fe/ZrO_2. It is conceivable that the deactivation of Cu(L) species is strongly suppressed by anchoring effects of the coexisting highly dispersed Fe_2O_3, probably due to the formation of Cu^0–Fe^{n+} ($n = 2,3$) bondings. It has been reported that the sinterings of Pt metal clusters encaged in zeolite cavities are significantly hindered in the presence of Fe^{2+} cations [28].

4. Conclusions

It was found that ZrO_2-supported Cu catalysts exhibited high activities and selectivities to N_2 for the NO–CO reaction at low temperature. Highly active Cu(L) species, which are formed by the reactions with the terminal OH groups on the ZrO_2 surface, are assigned to atomically dispersed Cu species. Cu(L) species were deactivated in two steps during the reaction. It is proposed that clusterings and subsequent agglomerations of atomically dispersed Cu^0 species take place during the reaction or under reducing conditions. It was found that the NO-treatments regenerated the deteriorated Cu/ZrO_2 at much lower temperature than the O_2-treatments. Cu–Fe/ZrO_2 catalysts were found to show significantly higher activities, selectivities, and stabilities for the NO–CO reaction than the component catalysts, indicating that catalytic synergies are generated between Cu and Fe supported on ZrO_2.

References

[1] F. Nakajima, Catal. Today, 10 (1991) 1.
[2] W.F. Egelhoff, Jr., in: D.A. King and D.P. Woodruff, Eds., Chemical Physics and Heterogeneous Catalysis, Vol. 4, Elsevier Science B.V., Amsterdam, 1982, p. 397.
[3] M. Funabiki, T. Yamada and K. Kayano, Catal. Today, 10 (1991) 33.
[4] A. Kudo, M. Steinberg, B.A. Bard, A. Campion, M.A. Fox, T. Mallouk, S.E. Webber and J.M. White, J. Catal., 125 (1990) 565.
[5] F. Boccuzzi, G. Ghiotti, A. Chiorino and E. Guglielminotti, Surf. Sci., 269/270 (1992) 514.
[6] M. Iwamoto and H. Hamada, Catal. Today, 10 (1991) 57.
[7] K. Tabata, J. Mat. Sci. Lett., 7 (1988) 147.
[8] H. Shimada, S. Miyama and H. Kuroda, Chem. Lett., (1988) 1797.
[9] N. Mizuno, H. Toyama, M. Tanaka, M. Yamamoto and M. Misono, Bull. Chem. Soc. Jpn., 64 (1991) 1383.
[10] N. Mizuno, M. Yamamoto, M. Tanaka and M. Misono, J. Catal., 132 (1991) 560.
[11] G.L. Bauerle, G.R. Service and K. Nobe, Ind. Eng. Chem. Prod. Res. Dev., 11 (1992) 54.
[12] Y. Okamoto, K. Ohto and T. Imanaka, Kagaku Kogaku Ronbunshu, 19 (1993) 863.
[13] F. Boccuzzi, E. Gulielminotti, G. Martra and G. Cerrato, J. Catal., 146 (1994) 449.
[14] W.-P. Dow and T.-J. Huang, J. Catal., 147 (1994) 322.
[15] K.A. Bethke, D. Alt and M.C. Kung, Catal. Lett., 25 (1994) 37.
[16] Y. Amenomiya, Appl. Catal., 30 (1987) 57.
[17] Y. Amenomiya I.T.A. Emesh, K.W. Oliver and G. Pleizier, in: M.J. Phillips and M. Ternan, Eds., Proc. 9th Int. Congress on Catalysis, Vol. 2, The Chemical Institute of Canada, 1988, p. 634.
[18] R.A. Koeppel, A. Baiker and A. Wokaum, Appl. Catal. A, 84 (1992) 77.
[19] Y. Nitta, O. Suwata, Y. Ikeda, Y. Okamoto and T. Imanaka, Catal. Lett., 26 (1994) 345.
[20] O. Suwata, Y. Ikeda, T. Fujimatsu, Y. Okamoto and Y. Nitta, Kagaku Kogaku Ronbunshu, 21 (1995) 1009.
[21] T. Yamaguchi, Y. Nakano and K. Tanabe, Bull. Chem. Soc. Jpn., 51 (1978) 3482.
[22] T. Yamaguchi, Sekiyu Gakkaishi, 36 (1993) 250.
[23] Y. Okamoto, H. Gotoh, H. Aritani, T. Tanaka and S. Yoshida, unpublished results.
[24] J. Leyrer, M.I. Zaki and H. Knözinger, J. Phys. Chem., 90 (1986) 4780.
[25] M. Margraf, J. Leyrer, E. Taglauer and H. Knözinger, Surf. Sci., 189/190 (1987) 842.
[26] H.F.J. van't Blik, J.B.A.D. von Zon, T. Huizinga, J.C. Vis, D.C. Koningsberger and R. Prins, J. Am. Chem. Soc., 107 (1985) 3139.
[27] T. Mizushima, K. Tohji, Y. Udagawa and A. Ueno, J. Phys. Chem., 94 (1990) 4980.
[28] M.S. Tzou, H. Jian and W.M.H. Sachtler, Appl. Catal., 20 (1986) 231.